Contribution from the Department of Inorganic Chemistry,
University of Umeå, S-901 87 Umeå, Sweden

Multicomponent Polyanions. 39. Speciation in the Aqueous H^+–MoO_4^{2-}–HPO_4^{2-} System As Deduced from a Combined Emf–^{31}P NMR Study†

Lage Pettersson,* Ingegärd Andersson, and Lars-Olof Öhman

Received October 29, 1985

Speciation in the molybdophosphate system has been studied by a combination of potentiometric (glass electrode) and ^{31}P NMR measurements at 25 °C in 3.0 M $Na(ClO_4)$ medium. Data cover the acidity range $5.5 > -\lg [H^+] > 0.5$.[1a] The total concentrations of molybdate, *Mo*, and phosphate, *P*, were varied within the limits $0.010 \le Mo \le 0.480$ M and $0.005 \le P \le 0.040$ M. By using the NMR data qualitatively and quantitatively, by adjusting formation constants to minimize deviations in both emf and NMR data, and by taking results from earlier complementary studies into consideration, we have now established the existence of 18 molybdophosphate complexes and been able to determine compositions and formation constants for the 14 different species that are formed in significant amounts (>0.05*P*). Four series of homonuclear molybdophosphate complexes exist. Besides the Mo_5P_2 and $Mo_{11}P$ series there are two isomeric Mo_9P series. In acid solutions ($-\lg [H^+] \lesssim 1.8$) and at high Mo/P ratios (>9) an $Mo_{12}P$ complex is present. Equilibria are rapid, except for $-\lg [H^+] < 3$, where the dimer $Mo_{18}P_2$ is slowly formed, the slower the higher the Mo/P ratio. This species takes up to 1 month to be formed in full amount. Equilibrium constants and NMR characteristics of the complexes formed are given. The equilibrium conditions for "fresh" and "aged" solutions are illustrated in distribution diagrams. Known and proposed structures of the main complexes are discussed.

Introduction

Attention was first given to molybdophosphates by Berzelius[1b] in 1826. Since then the system has been currently studied and a variety of compounds with many different Mo/P ratios has been reported. Many research groups had made considerable contributions to the chemistry of the molybdophosphates when we began to study the system in the late 1960s. However, knowledge about the number, the composition, and the structures of various species formed seemed incomplete.

Many reviews have also appeared; the most recent one is found in a book by Pope,[2] where he critically examines all representative papers on heteropoly- and isopolyanions published before the beginning of 1982. Species with Mo/P ratios of 2.5, 9, and 11 seem to be firmly established while the existence of the well-known Keggin ion, $Mo_{12}PO_{40}^{3-}$, is questioned in aqueous solution.

Recently we have, for solutions with $Mo/P \le 2.5$, verified the existence of the three species $H_nMo_5P_2O_{23}^{n-6}$ ($n = 0$–2), using a quantitative ^{31}P NMR technique.[3] The composition and stability found for these species showed full agreement with our earlier interpretation of potentiometric titration data.[4,5] In the same paper, however, it was also shown that at ratios above 2.5 between the total concentration of molybdenum(VI), *Mo*, and phosphorus(V), *P*, where the emf model had predicted a homonuclear series of enneamolybdophosphates, at least two species with different Mo/P ratios occur simultaneously. This had earlier been indicated in our combined potentiometric–spectrophotometric study of the system,[6] which pointed to at least two coexisting molybdophosphate series of different Mo/P ratios in slightly acidic solutions. The interpretation of these data was that, in addition to the predominating series of enneamolybdophosphates, Mo_9P, a minor series of undecamolybdophosphates, $Mo_{11}P$, existed simultaneously. Data were, however, found not to be decisive. A reinvestigation using a powerful complementary method seemed necessary. We decided to employ a combination of emf and quantitative ^{31}P NMR data with the aim of establishing the final speciation for the aqueous molybdophosphate system.

The study has been performed at 25 °C and in 3.0 M $Na(ClO_4)$ medium. The equilibria are written

$$p\mathrm{H}^+ + q\mathrm{MoO_4}^{2-} + r\mathrm{HPO_4}^{2-} \rightleftharpoons (\mathrm{H}^+)_p(\mathrm{MoO_4}^{2-})_q(\mathrm{HPO_4}^{2-})_r$$

and the formation constants are denoted as $\beta_{p,q,r}$. For brevity complexes formed are often given the notation (p,q,r), and homonuclear series are referred to by their (q,r) values.

† Parts of the present study were presented in a session lecture at the Climax Fifth International Conference on the Chemistry and Uses of Molybdenum, Newcastle upon Tyne, England, July 1985.

Experimental Section

Solutions and Analysis. All stock solutions ($NaClO_4$, $HClO_4$, Na_2MoO_4, and Na_2HPO_4) used were prepared and analyzed as described earlier.[4]

Emf Measurements. The measurements were carried out as a series of potentiometric titrations in 3.0 M $Na(ClO_4)$ medium at 25 °C. The emf equipment and arrangement as described earlier[4] were used. However, throughout the titration series the measurements were made with an automated potentiometric titrator.[7] The glass electrodes used were of the general-purpose type, Ingold 201-NS and Beckman 40498. They were tested against a hydrogen electrode and were found to give reliable values. The constant E_0, in the calculation of $-\lg [H^+]$ from the measured emf was determined separately in solutions with known $[H^+]$. This procedure is necessary since MoO_4^{2-} and HPO_4^{2-} take part in proton equilibria in all the $-\lg [H^+]$ regions studied. The determinations of E_0 were performed before and after each titration.

NMR Measurements. All ^{31}P NMR measurements were carried out on a Bruker WM-250 spectrometer equipped with a 10-mm multinuclear probe head. As instrumental lock, an inner concentric tube (i.d. = 1.5 mm) filled with D_2O, was used. To begin with, another capillary (o.d. = 0.5 mm) filled with 85% H_3PO_4 was inserted inside this tube in order to obtain a chemical shift standard. (The high-frequency-positive convention was used.) However, as two of the molybdophosphate peaks appeared very close to this standard, most spectra were recorded without internal standard. Instead, the NMR instrument was calibrated by running a separate spectrum of the standard before the measurements began.

All measurements were performed at 295 ± 1 K and, since rapid chemical exchange of the protons gave no multiplet structures, without proton irradiation. The spin–lattice relaxation times (T_1/s) of the different species, needed to perform quantitative measurements, were evaluated by using the inversion–recovery method. During the measurements, 90° pulses and scan repetition times larger than 5 times the longest T_1 present were used. Usually ($P = 0.020$ M) 64 scans were sampled (sampling time $\lesssim 1.5$ h) and the free induction decays were multiplied by an exponential line-broadening (1 Hz) function in order

(1) (a) Throughout this work, the term "lg" stands for $\log_{10}$, one of three recommendations of the IUPAC Commission on Symbols, Terminology and Units [*Pure Appl. Chem.* **1979**, *51*, 24 (decadic logarithm of *a*: lg *a*, $\log_{10}a$, log *a*)]. The present work performed under constant ionic strength involves calibration of the glass electrode against concentration of H^+. Thus we use $-\lg [H^+]$ rather than pH to distinguish our scale from the operationally defined NBS scale. (b) Berzelius, J. J. *Pogg. Ann.* **1826**, *6*, 369.
(2) Pope, M. T. *Heteropoly and Isopoly Oxometalates*; Springer: West Berlin and Heidelberg, 1983.
(3) Pettersson, L.; Andersson, I.; Öhman, L.-O. *Acta Chem. Scand., Ser. A* **1985**, *A39*, 53.
(4) Pettersson, L. *Acta Chem. Scand.* **1971**, *25*, 1959.
(5) Pettersson, L. *Chem. Scr.* **1975**, *7*, 145.
(6) Lyhamn, L.; Pettersson, L. *Chem. Scr.* **1980**, *16*, 52.
(7) Ginstrup, O. *Chem. Instrum.* (*N.Y.*) **1973**, *4*, 141.

0020-1669/86/1325-4726$01.50/0

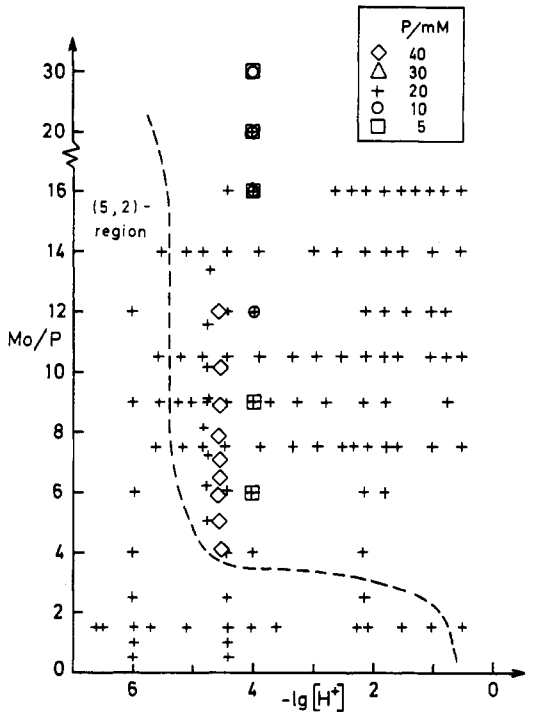

Figure 1. Points (*Mo*, *P*, -lg [H^+]) where NMR spectra have been recorded from "fresh" solutions. The (5,2) region, the part beneath the broken line, where only phosphates and Mo_5P_2 species are present, is indicated. This region was studied in ref 3.

to improve the signal/noise ratio. The concentration of phosphorus in a single peak was evaluated from its peak area, assuming that the sum of all areas was equal to the known total concentration of phosphorus in the sample. The instrument integrals could not be used for accurate quantitative analysis since, for example, the areas of small peaks were systematically underestimated. Instead, the areas were evaluated by multiplying the height and the full-width half-maximum values manually measured from expanded plots.

Description of Data

^{31}P NMR Data. In Figure 1, the different Mo/P ratios and -lg [H^+] ranges covered by this investigation are illustrated. First, a relatively coarse check pattern was created, and then, on the basis of the information obtained from these measurements, additional spectra were collected in the most interesting and informative areas. In the beginning, data were collected at several *P* levels, but as it was found that only minor information could be evaluated from these data, the vast majority of data were collected at $P = 0.020$ M.

As an example of experimentally obtained spectra, Figure 2 shows the result of a -lg [H^+] "titration" at $Mo/P = 10.5$ ($P = 0.020$ M). The information evaluated from these spectra comprises (i) the number of nonequivalent phosphate groups as a function of -lg [H^+], (ii) the ^{31}P NMR chemical shift value, δ, for each peak as a function of -lg [H^+] (cf. Figure 3), and (iii) the absolute amount of phosphorus bound in each peak.

In total, the data material comprises ≈100 spectra within the ranges $0.030 \le Mo \le 0.480$ M, $0.005 \le P \le 0.040$ M, and $0.5 \le$ -lg [H^+] ≤ 5.5.

As one of the species (peak H) was formed with extremely slow kinetics, repeated NMR spectra were recorded in this area until a constant time to time composition was obtained. Especially at Mo/P > 9, this equilibration time took almost 1 month.

Potentiometric Data. In the present study, the original data set from ref 4–6 has been used as a firm base. However, as this set of data contained very few data points in some areas of interest, a supplementary data material was also collected. No systematic differences between these sets of data were seen.

In addition, a batchwise determination of -lg [H^+] was performed in each of the solutions run for NMR spectra. This procedure was mainly intended to be a point of security, but it

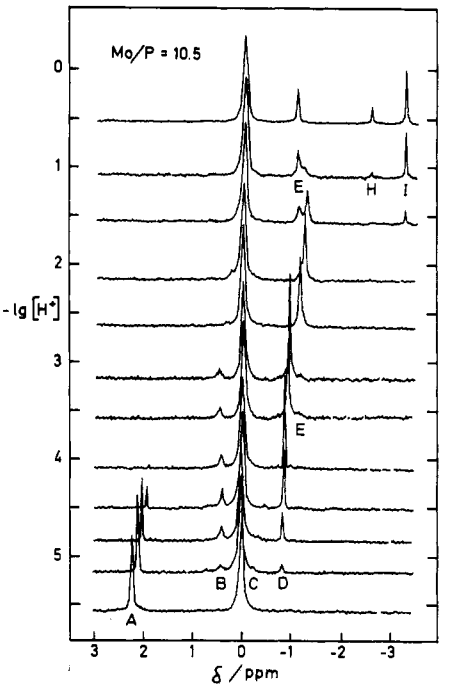

Figure 2. ^{31}P NMR spectra from a titration with $Mo = 210$ mM and $P = 20$ mM. The solutions are somewhat aged. The big peak at 0 ppm originates from the chemical shift standard, 85% H_3PO_4. Letters refer to the assignments in Table II.

Table I. Compilation of the Formation Constants for the Binary $(H^+)_p(MoO_4^{2-})_q$ and $(H^+)_p(HPO_4^{2-})_r$ and the Ternary $(H^+)_p(MoO_4^{2-})_5(HPO_4^{2-})_2$ Complexes Used As "Known" in the Calculations

(*p*,*q*,*r*)	tentative formula	lg $\beta_{p,q,r}$
(1,1,0)	$HMoO_4^-$	4.00
(2,1,0)	H_2MoO_4	7.50
(8,7,0)	$Mo_7O_{24}^{6-}$	57.699
(9,7,0)	$HMo_7O_{24}^{5-}$	62.140
(10,7,0)	$H_2Mo_7O_{24}^{4-}$	65.595
(11,7,0)	$H_3Mo_7O_{24}^{3-}$	68.344
(34,19,0)		196.3
(5,2,0)		19.0
(1,0,1)	$H_2PO_4^-$	6.244
(2,0,1)	H_3PO_4	8.096
(8,5,2)	$Mo_5P_2O_{23}^{6-}$	61.97
(9,5,2)	$HMo_5P_2O_{23}^{5-}$	67.07
(10,5,2)	$H_2Mo_5P_2O_{23}^{4-}$	70.86

also means that the potentiometric data set contains accurately determined -lg [H^+] data in the region where the slowly forming species (peak H) is formed in equilibrium amounts.

In total, the potentiometric data material collected since the late 1960s comprises about 2600 experimental points within the limits $0.0005 \le Mo \le 0.480$ M, $0.0002 \le P \le 0.080$ M, and $9 \ge$ -lg [H^+] ≥ 0.5. In the present study about one-fifth of this data material has been used.

Analysis of Data and Discussion

The general problem in an equilibrium analysis is to find a firm base from which the analysis can proceed. Another major problem, with indirect measurements such as potentiometry or spectrophotometry solely used, is to restrict the new data area in such a way that only one or at most two new species occur in the data set. These complications are, at least theoretically, largely overcome by employing NMR data. In these data, every unique chemical surrounding of the nucleus in question, being in slow exchange on the NMR time scale, gives rise to a unique NMR peak.

In the present system, we have earlier shown that, for Mo/P < 2.5 and -lg [H^+] > 1.5, the system is ^{31}P NMR characterized by the species $H_nPO_4^{n-3}$ ($n = 1$–3) and $H_n(MoO_4)_5(HPO_4)_2^{n-14}$

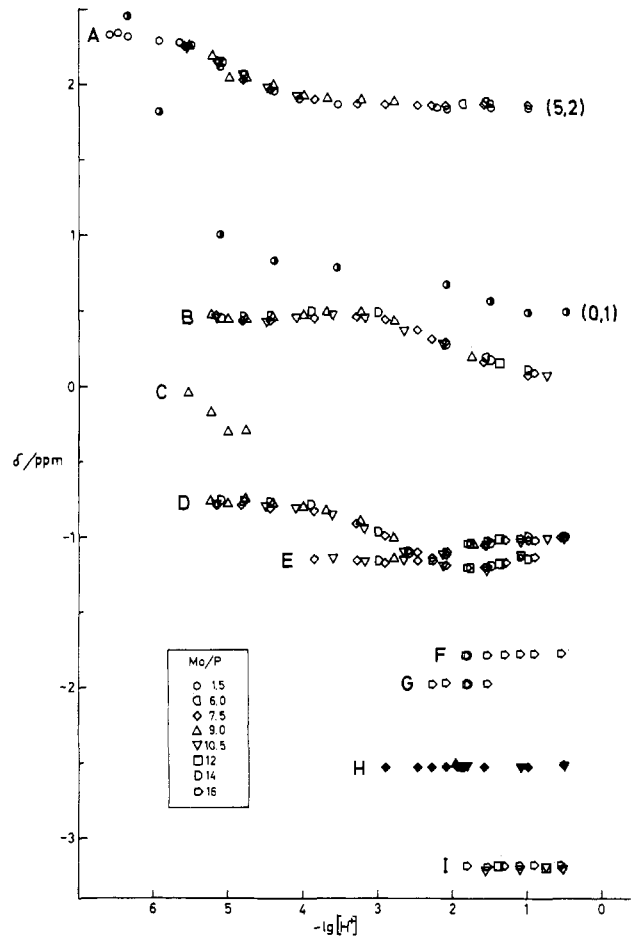

Figure 3. Chemical shifts, δ, as a function of $-\lg [H^+]$ for all different types of molybdophosphate species found. For comparison the phosphate shifts (from a titration with Mo/P = 1.5 (●)[3]) have been included. Letters refer to the assignments in Table II.

(n = 8–10), with equilibrium constants given in Table I. This comprises our firm base from which we will build our equilibrium analysis. In this analysis, graphical and stoichiometric evaluations of NMR data, least-squares calculations (LETAGROPVRID, version ETITR)[8] on emf data, and distribution calculations (SOLGASWATER)[9] on combined data will be intimately correlated. The final goal will be to find a model that minimizes deviations in both potentiometric *and* NMR measurements.

In Figure 3, the chemical shift values of all appearing peaks are shown as function of $-\lg [H^+]$. As seen, the system becomes increasingly complicated at decreasing $-\lg [H^+]$. Therefore it is logical to start the analysis from the neutral part of the system. In the range $5.5 \gtrsim -\lg [H^+] \gtrsim 3.9$, three "new" peaks appear. However, out of these, the peak denoted C never exceeds 5% of total phosphorus, and no effort will therefore be made to determine the composition of these species. Concerning the remaining two peaks, it was previously shown[3] that the species giving rise to the D peak was formed in larger amounts and had a higher Mo/P ratio than those giving rise to the B peak. As the position of these peaks is almost invariant for $-\lg [H^+] > 3.9$, we decided to test the assumption that each peak corresponds to a certain $(p,q,1)$ combination. This was performed as a stoichiometric test on 19 points with $4 \leq Mo/P \leq 30$ at $-\lg [H^+] = 4.0$.

In each point, the absolute concentration of phosphorus bound in $(p,5,2)$, $(p_1,q_1,1)$ (peak D), and $(p_2,q_2,1)$ (peak B) was known. Thus, the total concentration of binary molybdate species, $Mo^* = Mo - {}^5/_2[p,5,2] - q_1[p_1,q_1,1] - q_2[p_2,q_2,1]$, could be calculated. Multiplying this figure by Z_{Mo}, the known average number of protons bound per MoO_4^{2-} at $-\lg [H^+] = 4$, gave the amount of protons bound in binary molybdates. Z_{Mo} was calculated from the binary H^+–MoO_4^{2-} constants given in Table I and was found to be 1.24–1.27 (the higher the Mo^* the higher the Z_{Mo} value). The conditions for the total concentration of protons, H, then give: $H = [H^+] + Z_{Mo}Mo^* + p[p,5,2] + p_1[p_1,q_1,1] + p_2[p_2,q_2,1]$. Thus, with the assumption of a certain value of p_1, p_2 could be calculated as

$$p_2 = \frac{1}{[p_2,q_2,1]}(H - [H^+] - Z_{Mo}Mo^* - p[p,5,2] - p_1[p_1,q_1,1])$$

These calculations, systematically performed over all relevant integers of p_1, q_1, and q_2, showed q_1 to be uniquely set to 11, as higher values resulted in negative Mo^* values and lower values resulted in unrealistically high internal acidities ($p_2/q_2 > 2$) in the minor species. For this latter reason, it was also found that the value of p_1 had to be very close to 18. As to the minor species, it could, however, not be deduced whether the composition was (10,6,1), (11,7,1), (13,8,1), or (14,9,1). (q_2 = 10 resulted in negative Mo^* values.)

The next step in data analysis was therefore a series of LETAGROP calculations on potentiometric data with $-\lg [H^+] \geq 4$. In these calculations, the formation constant for each of the alternative species was varied together with the formation constant for (18,11,1). The result of these calculations was that none of the pairs considered could explain the whole data set. Especially in the region $5.0 \leq -\lg [H^+] \leq 5.5$, considerable deviations between measured and calculated $-\lg [H^+]$ values were obtained.

Despite the relative invariance in peak position for the two peaks, we therefore found it necessary to test if emf data could be explained by including (17,11,1) and $(p_2 \pm 1,q_2,1)$ into the model. These renewed calculations, now performed in the range $3.9 \leq -\lg [H^+] \leq 5.0$ to avoid the eventual influence from the minor C species, previously mentioned, showed that an excellent fit to data now could be obtained. However, a definite speciation could not be established as all four combinations (10,6,1), (11,7,1) + (12,7,1), (13,8,1), and (14,9,1) + (15,9,1) together with (17,11,1) + (18,11,1) explained the experimental data almost equally well.

The only remaining possibility to distinguish between these alternatives was to return to the NMR measurements. Through these measurements, the distribution of (11,1):s vs. $(q_2,1)$:s was known at different Mo/P ratios and $-\lg [H^+]$ values. When the corresponding distribution curves for the emf alternatives were calculated, it was found that only (14,9,1) + (15,9,1) and the (11,1):s were consistent with the NMR data. All lower values in q_2 gave as result that the maximum amount of the minor species occurred at Mo/P ratios that were too low. Thus, on the basis of the combined information obtained from the two methods, the speciation in the range $Mo/P > {}^5/_2$, $-\lg [H^+] > 3.9$, could be uniquely determined as (17,11,1) + (18,11,1), peak D, and (14,9,1) + (15,9,1), peak B.

At $-\lg [H^+] \approx 3.9$ an additional peak, E, appears. At the same time, both the (11,1) and the (9,1) peaks start to move with $-\lg [H^+]$. Thus, we can expect that additional protons are being attached. In order to evaluate the nuclearity in the additional peak, we decided to record a series of NMR spectra with varying Mo/P ratio. When choosing the $-\lg [H^+]$ value for this "titration" one has to consider that the peaks D and E intersect at $-\lg [H^+] \approx 2.3$. Therefore, up to half a logarithmic unit on each side the peak overlap will make individual area determinations difficult. At $-\lg [H^+] \gtrsim 2.8$ the E peak is a minor peak, which is not the case for $-\lg [H^+] \lesssim 1.8$. However, at this more acid value the speciation is more complex as small amounts of species, giving rise to the F, G, and I peaks will be present at high Mo/P ratios (cf. Figure 3). Nevertheless, we decided to collect data on the acid side of the intersection. The distribution of phosphorus in the main peaks from the titration at $-\lg [H^+] = 1.8$ is shown in Figure 4. The quotient between the areas of the B peak (the (9,1) species) and the new E peak is constant throughout the entire Mo/P range. It can thus be established that the E peak is also caused by a (9,1) species (from now on denoted (*9,1) to dis-

(8) Arnek, R.; Sillén, L.-G.; Wahlberg, O. *Ark. Kemi* **1969**, *31*, 353. Brauner, P.; Sillén, L.-G.; Whiteker, R. *Ark. Kemi* **1969**, *31*, 365.
(9) Eriksson, G. *Anal. Chim. Acta* **1979**, *112*, 375.

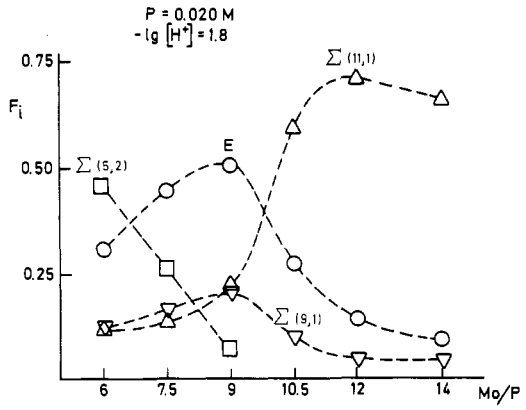

Figure 4. Recorded distribution of phosphorus (in main peaks) as a function of Mo/P at $-\lg [H^+] = 1.8$.

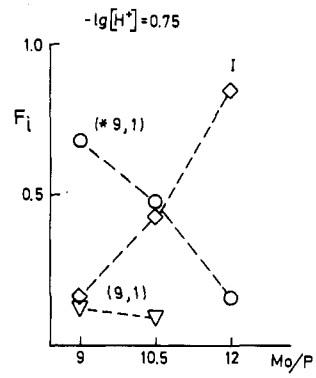

Figure 5. Recorded distribution of phosphorus as a function of Mo/P at $-\lg [H^+] = 0.75$.

tinguish the two isomers). This finding was further confirmed by the emf data, now extended down to $-\lg [H^+] = 1.5$, as these were well explained when the species (19,11,1), (16,9,1), and (17,9,1) were included in the model, although some small systematic deviations still remained in the most acid region.

Thus, two different species of (9,1):s with differing magnetic environments around the phosphorus atom are existing simultaneously. To our knowledge, such a phenomenon has never been experimentally proved before, even if speculations based on geometrical considerations have suggested that such phenomena should be possible.

Going to still lower $-\lg [H^+]$, i.e. $-\lg [H^+] < 1.5$, NMR spectra demonstrate the presence of a fourth additional major peak, I. Figure 5, which illustrates a Mo/P NMR "titration" at $-\lg [H^+] = 0.75$, shows that the Mo/P ratio in this species is higher than 9 as it strongly dominates the (9,1) complexes at high ratios. Other Mo/P ratio titrations at somewhat lower acidities ($-\lg [H^+] = 1$–1.5), where $Mo_{11}P$ species are present, showed that the Mo/P ratio must be greater than 11.

As a complex with the composition (23,12,1) can be precipitated from acid solutions having high Mo/P ratios, it was logical to test whether peak I was caused by this species. This test was performed on 15 NMR spectra in the region $9 \leq Mo/P \leq 16$, $0.5 \leq -\lg [H^+] \leq 1.5$, and it was found that, when $\lg \beta_{23,12,1} = 139.7$ was applied, the calculated amount of (12,1) fully coincided with those measured in all 15 spectra. The uncertainty in this formation is estimated to be ±0.1 logarithmic unit. When this additional species was included in the model, emf data were fully explained and the systematic deviations mentioned above had disappeared.

As already mentioned two minor peaks, F and G, appear in the acid range (cf. Figure 3). The chemical shift values for these peaks show no $-\lg [H^+]$ dependence, thus indicating that each peak originates from a single complex. However, as less than 5% of P_{tot} was found to be bound in these species no attempts were made to evaluate their definite compositions. From present data it can, however, be deduced that their Mo/P ratios are even higher than 12. They are thus favored in solutions having the highest

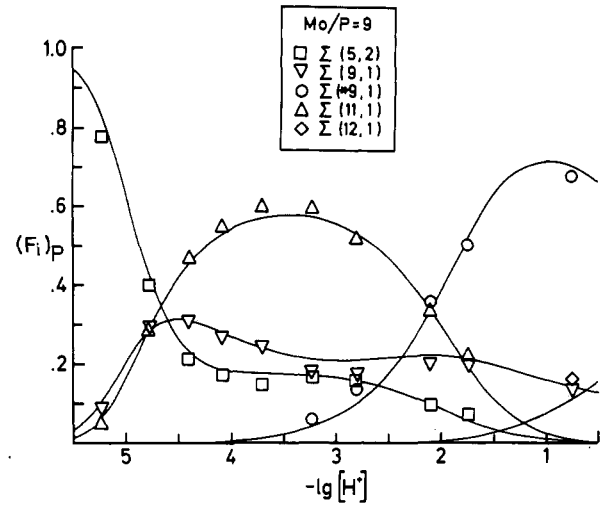

Figure 6. Diagram showing the distribution of phosphorus in homonuclear series as a function of $-\lg [H^+]$. The symbols represent experimental NMR points and the fully drawn curves have been calculated by using the constants in Tables I and II.

Mo/P ratios. Such solutions are, on the other hand, not stable as binary molybdate phases precipitate after some time. It is therefore difficult to obtain conditions where their compositions and stabilities could be accurately determined.

The nuclearities of the species in the main peaks A, B, D, E, and I, all seem to be well established. However, to obtain the "best" set of equilibrium constants, both emf and NMR data should be taken into account. After a tedious work adjusting formation constants and comparing the resulting calculated amounts with experimentally determined ones to obtain the "best" combined fit, the set given in Table II was obtained. In Table III the old emf and the final emf–NMR model on a representative potentiometric data set are compared. As seen the error squares sum, U, has diminished by a factor of 3 when the new model is used. Concerning the isomeric (16,9,1) and (17,9,1) species, emf data can only give the sum of the formation of these species. The values given in Table III therefore refer to (16,9,1) + (*16,9,1) and (17,9,1) + (*17,9,1), respectively. The very existence of this isomerism, as well as the individual formation constants for these species can only be established from NMR data. In the table are also compiled two of the many LETAGROP calculations that have been performed in the search for the final model. In calculation no. 1, the β values for the four Mo_9P species and the (23,12,1) complex were varied while the $Mo_{11}P$ species had their fixed final values. In calculation no. 2 the β values of the three $Mo_{11}P$ species were varied but not those of the others. In both calculations the U values are somewhat lower than in the final model. Although these β values do not differ much from those in the final, combined, set, the fit to NMR data is significantly affected.

As mentioned before, the adjustment of formation constants to obtain the "best" combined fit has been very laborious. Every new model has had to be tested against the NMR data. This has been performed by plotting the calculated amount of phosphorus bound in different homonuclear series (or single species) for different titrations and then comparing these plots with the experimental amount found in each NMR peak. An example of such a plot is given in Figure 6 for a $-\lg [H^+]$ titration at $Mo/P = 9$ ($P = 0.020$ M). The experimental points are in good accordance with the calculated distribution obtained when the final emf–NMR model given in Table II is used. All the other $-\lg [H^+]$ and Mo/P ratio titrations show a corresponding good fit. The only small systematic deviations found are in regions where the minor peaks C, F, and G exist.

So far, only equilibria in fresh solutions have been treated but, as mentioned before, the species that gives rise to the H peak is formed very slowly. No sign of the peak was found in solutions less than 24 h old, and the complex thus did not need to be taken into consideration in such "fresh" solutions.

Table II. Final Combined Emf-NMR Model[a]

NMR assignm.	(p,q,r) notation	lg $\beta_{p,q,r}$	pK_a	Formula	Structure	Ref.
A	8,5,2	61.97(2)		$Mo_5P_2O_{23}^{6-}$	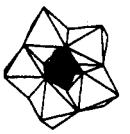	11, 12
	9,5,2	67.07(5)	5.10	$HMo_5P_2O_{23}^{5-}$		13
	10,5,2	70.86(8)	3.79	$H_2Mo_5P_2O_{23}^{4-}$		14
B	14,9,1	98.21(7)				
	15,9,1	102.04(8)	3.83			
	16,9,1	104.89(8)	2.85			
	17,9,1	106.42(8)	1.53			
E	*16,9,1	104.71(8)		$Mo_9PO_{31}OH(OH_2)_2^{4-}$	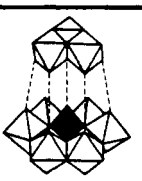	15,16
	*17,9,1	107.17(5)	2.46	$Mo_9PO_{31}(OH_2)_3^{3-}$		
H	34,18,2	217.8 (1)		$Mo_{18}P_2O_{62}^{6-}$	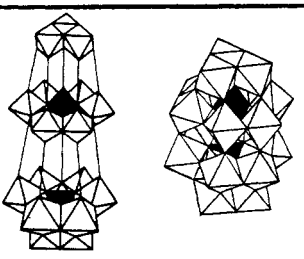	17
D	17,11,1	118.68(8)		$Mo_{11}PO_{39}^{7-}$	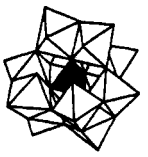	
	18,11,1	123.10(5)	4.42	$HMo_{11}PO_{39}^{6-}$		
	19,11,1	126.05(5)	2.95	$H_2Mo_{11}PO_{39}^{5-}$		
I	23,12,1	139.7 (1)		$Mo_{12}PO_{40}^{3-}$	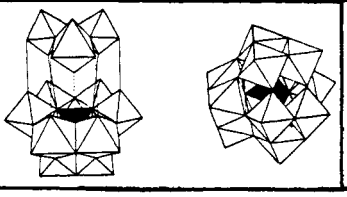	18

[a] The figures in parentheses are estimated uncertainties and refer to the last decimal place given. The structures A, E, H, and I are known and those of B and D are proposed.

Table III. Results from Some LETAGROP Calculations on Fresh Data in the Range $5 > -\lg [H^+] > 1.5$[a]

	old emf model	final emf-NMR model	calcn 1	calcn 2
$10^{-2}U$[b]	8.74	2.95	2.64	2.38
$\sigma(H)$	1.95	1.13	1.08	1.02
(14,9,1)	98.40	98.21	98.30 (7)	98.21
(15,9,1)	102.81	102.04	101.93 (22)	102.04
(16,9,1)	105.84	105.11	105.12 (20)	105.11
(17,9,1)	106.85	107.24	107.20 (11)	107.24
(17,11,1)		118.68	118.68	118.65 (7)
(18,11,1)		123.10	123.10	123.03 (3)
(19,11,1)		126.05	126.05	125.97 (5)
(23,12,1)		139.70	139.80 (10)	139.70

[a] Data consist of 25 titrations and 233 experimental points. The 3σ values given in parentheses refer to the last decimal place given. The binary constants and the Mo_5P_2 constants used in the calculation are compiled in Table I. [b] U is defined as $\sum(H_{calcd} - H_{exptl})^2$.

In a Raman study of the system[10] we recorded spectra both from the solid phases $Na_3Mo_9PO_{31}(OH_2)_3(H_2O)_{12-13}$ and $Na_6Mo_{18}P_2O_{62}(H_2O)_{24}$ and from fresh aqueous solutions of the dissolved phases. A comparison of these spectra with those of fully equilibrated $(H^+)_{16}(MoO_4^{2-})_9(HPO_4^{2-})$ and $(H^+)_{17}(MoO_4^{2-})_9(HPO_4^{2-})$ solutions revealed that the first solution contains both the Mo_9P and the $Mo_{18}P_2$ species and that the dimer is predom-

(10) Lyhamn, L.; Pettersson, L. *Chem. Scr.* **1977**, *12*, 142.
(11) Strandberg, R. *Acta Chem. Scand.* **1973**, *27*, 1004.
(12) Hedman, B. *Acta Crystallogr., Sect. B: Struct. Crystallogr. Cryst. Chem.* **1977**, *B33*, 3083.
(13) Hedman, B.; Standberg, R. *Acta Crystallogr., Sect. B: Struct. Crystallogr. Cryst. Chem.* **1979**, *B35*, 278.
(14) Hedman, B. *Acta Chem. Scand.* **1973**, *27*, 3335.
(15) Strandberg, R. *Acta Chem. Scand., Ser. A* **1974**, *A28*, 217.
(16) Hedman, B. *Acta Chem. Scand., Ser. A* **1978**, *A32*, 439.
(17) Strandberg, R. *Acta Chem. Scand., Ser. A* **1975**, *A29*, 350.
(18) Strandberg, R. *Acta Chem. Scand., Ser. A* **1975**, *A29*, 359.

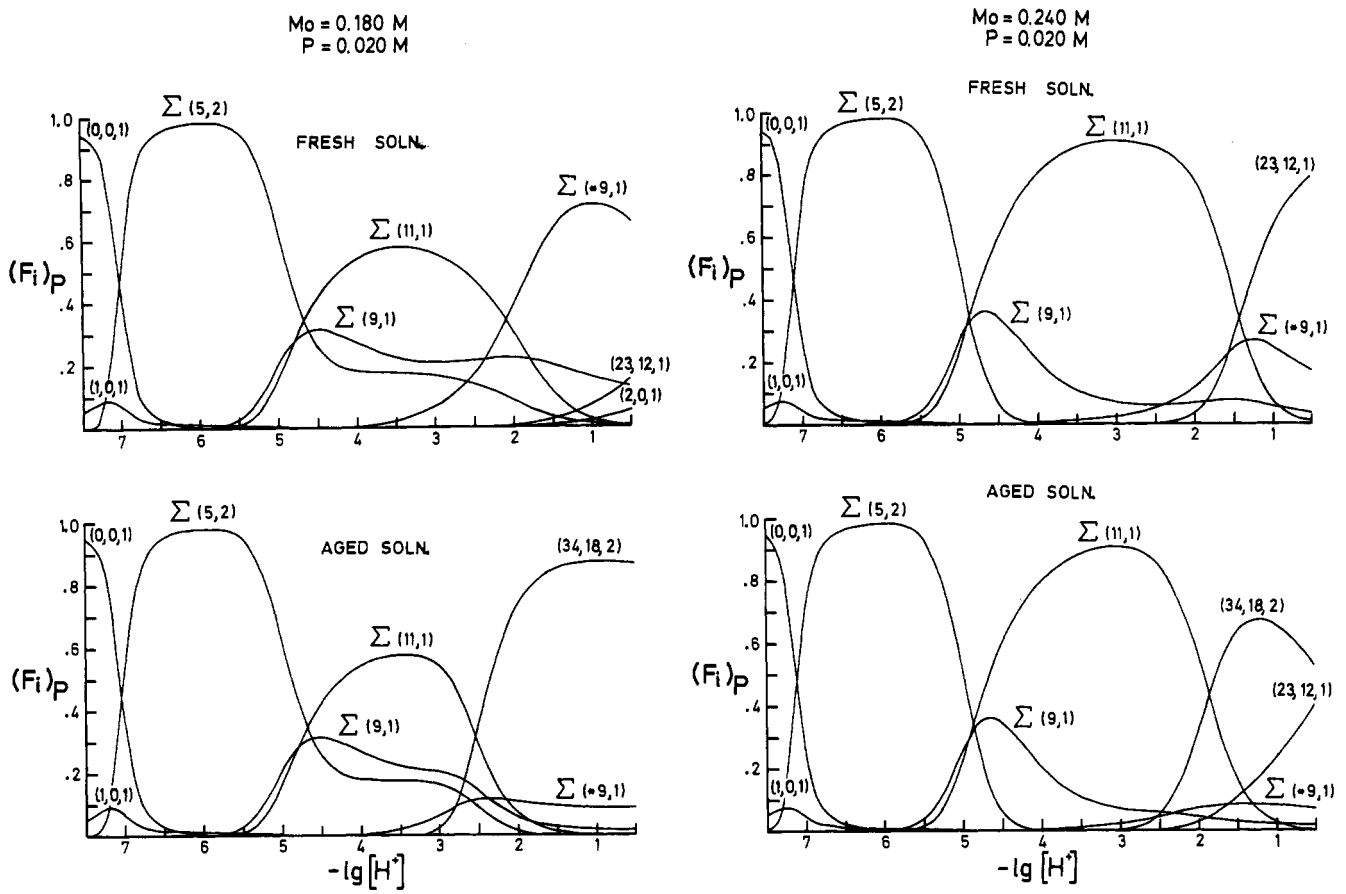

Figure 7. Diagrams showing the distribution of P-containing species at the Mo/P ratios 9 and 12 in fresh and aged solutions. Observe that for homonuclear molybdophosphate series the sum of and not the amounts of individual species are illustrated. The quantity $(F_i)_P$ is defined as the ratio between phosphorus in a species (or sum of homonuclear species) to total phosphorus. In the calculations the constants given in Tables I and II were used.

inant in the second solution. We therefore feel quite confident that the H peak originates from the $Mo_{18}P_2O_{62}^{6-}$ anion, (34,18,2) in (p,q,r) notation. To elucidate the equilibrium conditions in aged solutions we recorded NMR spectra of 18 solutions in the range $-\lg [H^+] < 3$ until no further changes in the peak areas were detected. In some cases, especially at Mo/P $\gtrsim$ 12, precipitation occurred before equilibria were attained. In the evaluation of the formation constants, the $\beta_{34,18,2}$ value was gradually changed until the calculated amount of the (34,18,2) complex was in accordance with the NMR spectra of aged stable solutions. The "best" lg $\beta_{34,18,2}$ value was found to be 217.8 with an estimated uncertainty of 0.1.

The molybdophosphate system is without doubt very complicated. One can certainly not get a view of the equilibrium conditions just by looking at the formation constants. With the aid of the computer program SOLGASWATER,[9] we have therefore constructed some distribution diagrams. In the diagrams in Figure 7 we have, due to the complexity of the system, chosen to show just the sum of species in homonuclear series. The upper diagrams illustrate conditions in fresh solutions, which are metastable at $-\lg [H^+] < 3$. As seen, the distribution of complexes is very sensitive to the Mo/P ratio. Thus, an increase from 9 to 12 greatly enhances the amount of (23,12,1) and the (11,1):s formed. In aged solutions, the dimer (34,18,2) is formed at $-\lg [H^+] < 3$, causing big changes in the chemical speciation as shown in the lower diagrams in Figure 7. The strength of this complex is demonstrated by the fact that it is quite predominant at $-\lg [H^+] < 2.5$ at Mo/P = 9 and that more than 50% of P is bound in the dimer in the range $1.8 > -\lg [H^+] > 0.5$ at Mo/P = 12. To show all the members in the different series we have constructed another type of distribution diagram, exemplified in Figures 8 and 9. In Figure 8 the distribution of species is shown for both fresh and aged solutions at Mo/P = 6 and 9. These diagrams, although just showing phosphorus-containing species, clearly demonstrate the complexity of the system. In Figure 9 the equilibrium conditions in aged solutions at Mo/P = 12 are illustrated. The left diagram shows the distribution of Mo-containing species, and the right diagram, P-containing species. As the ^{31}P NMR data have been of such tremendous help in solving the speciation, we have chosen to construct most diagrams to show P-containing species. It must, however, be borne in mind, that isopolymolybdate species, although not shown, may also be present. These are only to be found in diagrams showing Mo-containing species. Thus both types of diagrams, as exemplified in Figure 9, are needed to get a complete representation of the speciation. The right diagrams in Figure 7 clearly demonstrated that the initially high concentration of the (12,1) complex in fresh acid Mo/P = 12 solutions diminished considerably when the (18,2) complex was formed. That the liberated Mo causes the concentration of isopolymolybdate species to increase is shown in the left diagram of Figure 9.

Structural Comments. We have considered the molybdophosphate system very interesting from a structural point of view and have therefore spared no efforts trying to determine the structures of the species. As stated before six main peaks, A, B, D, E, H, I, are to be found in the system. Two of the peaks, H and I, originate from single species and the other from species in homonuclear series having two to four members (see Table II). The structures of the single species (34,18,2), peak H, and (23,12,1), peak I, as well as all the three species (8,5,2), (9,5,2) and (10,5,2), peak A, and the predominant enneamolybdophosphate species (*17,9,1), peak E, have all been determined by X-ray crystallography. The formulas and references for the structural determinations (only those performed at our department) are given in Table II. The polyhedron structures of the anions are illustrated as well. The single proton in the (9,5,2) structure and the two protons in the (10,5,2) structure are attached to the apex oxygens of the phosphate tetrahedra. The (*17,9,1)

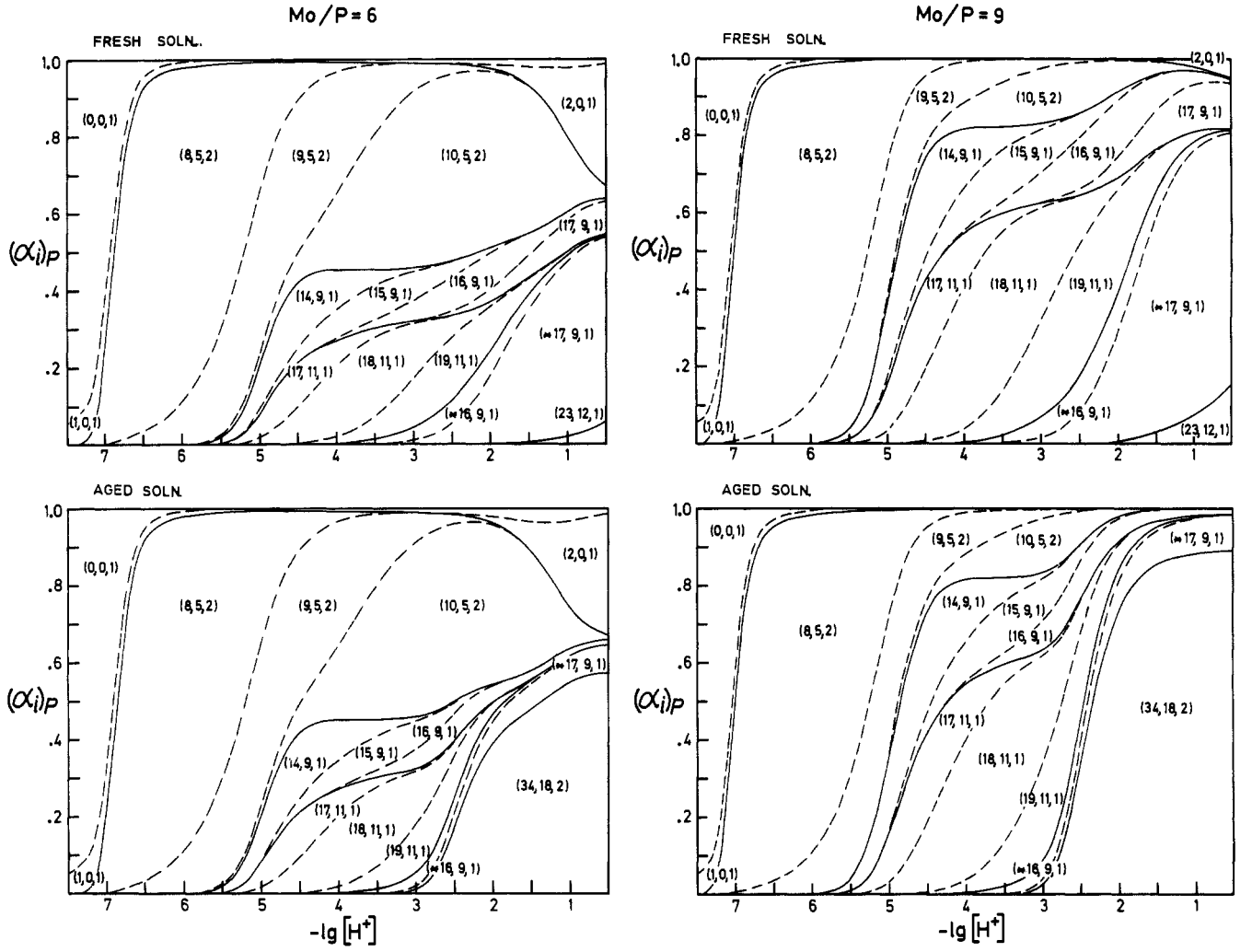

Figure 8. Distribution diagrams showing all P-containing species in fresh and aged solutions for the Mo/P ratios 6 and 9 at $P = 20$ mM. The quantity α_i is defined as the ratio between phosphorus in a species to total phosphorus. The species are added to each other, which means that the distribution of a single species should be vertically measured between two lines. The constants given in Tables I and II were used in the calculations.

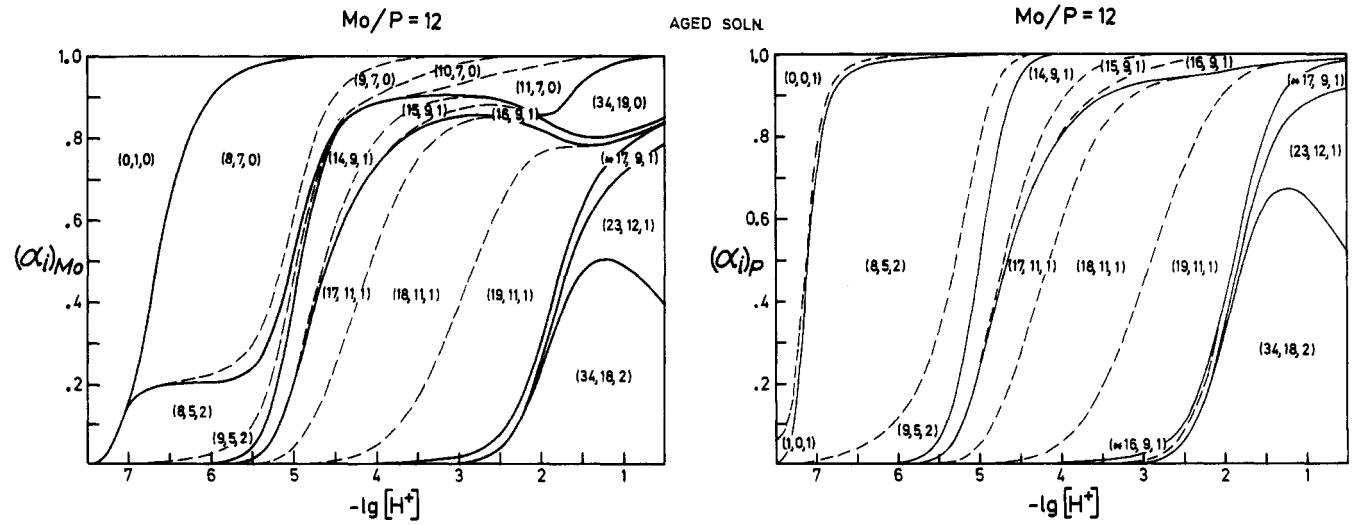

Figure 9. Diagrams showing the distribution of Mo-containing species (left) and P-containing species (right) for aged solutions at Mo/P = 12 and $P = 20$ mM. The quantity of α_i is defined as in Figure 8. The constants given in Tables I and II were used in the calculations.

anion has the so-called α-A structure where every second apex Mo–oxygen pointing downwards in the figure is a water oxygen. As the (*16,9,1) species has one proton less, it is reasonable to assume that one H_2O has lost one of its protons. This may be hard to prove experimentally. Being a minor species (cf. Figure 8) it will certainly turn out to be difficult to obtain single crystals containing isolated (*16,9,1) units.

Two structures, those of the complexes giving rise to peaks B and D, still have to be solved. The three (11,1) species, peak D, most probably have the lacunary Keggin structure shown in Table II. If so, the first member in the series (17,11,1) has the formula $Mo_{11}PO_{39}^{7-}$ with no protons attached. The second member (18,11,1) has been isolated as the unstable ammonium salt $(NH_4)_6Mo_{11}PO_{38}(OH)$.[19] For the four (9,1) species, peak B, we

propose the so-called α-B (9,1) structure shown in Table II. The downfield ^{31}P chemical shift value of the B peak, the (9,1) species, compared to that of the E peak, the (*9,1) species, which have the α-A (9,1) structure, is consistent with this proposal. To our knowledge the α-B structure has not yet been found as isolated units in crystals but has been found as moieties in some tungstophosphatocobaltates.[20,21] Recently, a B-type W_9P has been identified by Knoth et al.[22] by means of solid-state ^{31}P NMR measurements (chemical shift anisotropy). They have concluded that the A-type W_9P upon thermolysis converts to a B-type isomer.

To ascertain that the structures of the anions in solution are the same as those found as isolated units in crystalline phases two large-angle X-ray scattering (LAXS) studies on concentrated solutions have earlier been performed. In the first the three pentamolybdodiphosphate complexes were studied.[23] No significant differences in the structures or in the intraatomic distances between complexes in crystals and in solution could be detected. In the second, two enneamolybdomonophosphate solutions $(H^+)_{15}(MoO_4^{2-})_9(HPO_4^{2-})$ and $(H^+)_{16}(MoO_4^{2-})_9(HPO_4^{2-})$ with Mo = 1.6 M were studied.[24] It was found that the complexes in solution had the same basic structure as $Mo_9PO_{31}(OH_2)_3^{3-}$, the (*17,9,1) complex (Table II). Differences in the intraatomic distances were, however, established. A better agreement between observed and calculated shape functions was obtained when the zigzagged ring of six MoO_6 octahedra was flattened and somewhat enlarged. In the (16,9,1) solution there were moreoever indications that part of the molybdenum occurred as larger complexes, probably the (18,2) dimer.

The present study has revealed that (9,1) species are certainly not predominant in aged solutions having a Mo/P ratio of nine (cf. Figure 8). A recalculation of LAXS data using the final equilibrium model is in progress. Preliminary results have thereby shown the LAXS data to be in full accordance with the equilibrium constants and the structures given in Table II. It should, however, be noted that LAXS data are not particularly decisive when the solution contains two or more complexes having similar structures. In the present system, this is the case for the (9,1), (*9,1), and (11,1) complexes (B, E, and D peaks), which are all closely related to the (12,1) Keggin structure (peak I).

Crystallization experiments using a variety of cations are in progress. In these experiments, the polarity of the solvent is also varied by the addition of different organic liquids. We also intend to use a monosubstituted organic phosphate in the crystallization experiments. With such a three-dentate phosphate group, the α-B (9,1) species (as proposed for the B peak) should be formed, while the formation of both the α-A (9,1) species (peak E) and the lacunary (11,1) species (peak D) should be hindered. Thus, with such a central group, the α-B (9,1) species should be greatly favored and therefore easy to precipitate.

Conclusions

Through the present study the molybdophosphate system has been shown to be much more complicated than was earlier thought. Although we had previously studied the system for a long time using a variety of experimental methods, it is first by using the very powerful combination of potentiometry and ^{31}P NMR that we have succeeded in solving the speciation. The evaluation of the combined data has been very tedious and laborious. No doubt there is a great need of a computer program designed to treat combined emf–NMR data. In fact, the development of such a program has already been started at our department.

Table IV. ^{31}P NMR Characteristics for Different Molybdophosphate Complexes

NMR assignt	(p,q,r)	δ vs. 85% H_3PO_4	$\nu_{1/2}$/Hz	T_1/s
A	(8–10,5,2)	2.35–1.86	3.5–4.5–2.9	3
B	(14–17,9,1)	0.47–0.08	8.2–4.3	11
D	(17–19,11,1)	−0.78 to −1.20	4.3	13
E	(*16–17,9,1)	−1.15 to −1.00	4.3	14
H	(34,18,2)	−2.53	2.9	14
I	(23,12,1)	−3.20	2.9	30

The results from our equilibrium analyses of the system are summarized in Table II, and the NMR characteristics for the different species are given in Table IV. In addition to the complexes given in Table II, NMR data have established the existence of additional minor species constituting peaks C, F, and G in Figure 3. Within the concentration ranges presently studied, none of these bind more than 5% of total phosphorus. Furthermore, they all have a rather restricted range of existence (cf. Figure 3). Therefore, no efforts were made to determine their compositions. However, NMR data indicates that peak C originates from at least two species in fast protonation equilibria with each other having a Mo/P ratio of about 9 and that the peaks F and G originate from species having Mo/P ratios > 12.

Concerning the major species, we are confident that the model proposed in Table II is essentially correct. Of the main series, the (14-17,9,1) species, peak B, have been the hardest to establish and have therefore been thoroughly tested. A series of Mo_8P species explains emf data almost equally well. NMR data have, however, strongly supported the (9,1) series. Concerning the values of the β constants, we have tried to estimate the uncertainties and these are given in the table. A calculation in the future using a computer program adapted for combined emf–NMR data might change the formation constants somewhat, perhaps to one-tenth in the logarithmic value.

Known and proposed structures of the main species are illustrated in Table II. Those of the complexes giving rise to peaks B and D still have to be proved. The proposed lacunary (9,1) and (11,1) structures shown in the table seem, however, very plausible and are moreover in accordance with LAXS data (see above).

The equilibria in this complicated system are surprisingly rapid with one outstanding exception, the formation of the $Mo_{18}P_2$ dimer. The slow formation of this complex is very puzzling as the $*Mo_9P$ monomers are present in significant amounts and the structures of the monomer and the dimer indicate that the dimerization is a simple condensation reaction

$$2Mo_9PO_{31}(OH_2)_3^{3-} \rightleftharpoons Mo_{18}P_2O_{62}^{6-} + 6H_2O \qquad \lg K = 3.5$$

without any structural rearrangement.

Acknowledgment. We thank Professor Nils Ingri for his great interest, his valuable advice, and all the facilities placed at our disposal, the members of the NMR group at the Department of Organic Chemistry, Umeå University, for being in charge of the Bruker NMR apparatus, Christina Broman for typing the manuscript, and Lage Bodén for drawing the figures. This work forms part of a program financially supported by the Swedish Natural Science Research Council.

(19) Fournier, M.; Massart, R. *C. R. Seances Acad. Sci., Ser. C.* **1974**, *279*, 875.
(20) Weakley, T. J. R.; Evans, H. T., Jr.; Showell, J. S.; Tourné, G. F.; Tourné, C. M. *J. Chem. Soc., Chem. Commun.* **1973**, 139.
(21) Weakley, T. J. R. *J. Chem. Soc., Chem. Commun.* **1984**, 1406.
(22) Knoth, W. H.; Domaille, P. J.; Farlee, R. D. *Organometallics* **1985**, *4*, 62.
(23) Johansson, G.; Ingri, N.; Pettersson, L. *Acta Chem. Scand., Ser. A* **1974**, *A28*, 1119.
(24) Johansson, G.; Ingri, N.; Pettersson, L. *Acta Chem. Scand., Ser. A* **1978**, *A32*, 407.